

# The Progenitors of the Milky Way Stellar Halo: Big Bricks Favoured over Little Bricks

A. J. Deason<sup>\*1,4</sup>, V. Belokurov<sup>2</sup>, D. R. Weisz<sup>3,4</sup>

<sup>1</sup>*Department of Astronomy and Astrophysics, University of California Santa Cruz, Santa Cruz, CA 95064, USA*

<sup>2</sup>*Institute of Astronomy, University of Cambridge, Madingley Road, Cambridge, CB3 0HA, UK*

<sup>3</sup>*Astronomy Department, University of Washington, Seattle, WA 98195, USA*

<sup>4</sup>*Hubble Fellow*

10 September 2021

## ABSTRACT

We present a census of blue horizontal branch (BHB) and blue straggler (BS) stars belonging to dwarf galaxies and globular clusters, and compare these counts to that of the Milky Way stellar halo. We find, in agreement with earlier studies, that the ratio of BS-to-BHB stars in these satellite populations is dependent on stellar mass. Dwarf galaxies show an increasing BS-to-BHB ratio with luminosity. In contrast, globular clusters display the reverse trend, with  $N_{\text{BS}}/N_{\text{BHB}} (\lesssim 1)$  decreasing with luminosity. The faintest ( $L < 10^5 L_{\odot}$ ) dwarfs have similar numbers of BS and BHB stars ( $N_{\text{BS}}/N_{\text{BHB}} \sim 1$ ), whereas more massive dwarfs tend to be dominated by BS stars ( $N_{\text{BS}}/N_{\text{BHB}} \sim 2 - 40$ ). We find that the BS-to-BHB ratio in the stellar halo is relatively high ( $N_{\text{BS}}/N_{\text{BHB}} \sim 5 - 6$ ), and thus inconsistent with the low ratios found in both ultra-faint dwarfs and globular clusters. Our results favour more massive dwarfs as the dominant “building blocks” of the stellar halo, in good agreement with current predictions from  $\Lambda$ CDM models.

**Key words:** Galaxy: formation — Galaxy: halo — galaxies: dwarf.

## 1 INTRODUCTION

The Milky Way is a cannibal; throughout its lifetime it captures and destroys smaller dwarf galaxies. The remains of destroyed dwarfs are splayed out in a diffuse stellar halo, while the dwarfs evading destruction comprise the satellite population that orbits the Galaxy. Despite this well-established, generic picture of stellar halo formation, we have very little understanding of what the building blocks of the halo actually are; is the halo built up from many small mass tidbits, or from one (or two) massive dwarf(s)?

The chemical properties of halo stars have often been used to connect them to their progenitor galaxies. For example, the relation between  $[\alpha/\text{Fe}]$  and  $[\text{Fe}/\text{H}]$  is an indicator of the rate of self-enrichment, and therefore can be linked to the host galaxy’s mass. However, the  $[\alpha/\text{Fe}]$  abundances of halo stars appear to differ significantly from those of the (classical) dwarf galaxy satellites in the Milky Way (Tolstoy et al. 2003; Venn et al. 2004), whereby the halo stars are typically more  $\alpha$ -enhanced at a given metallicity. Thus, there is little evidence for the accretion of fragments similar to the present-day dwarf spheroidal population.

The mismatch in chemical properties between the bulk of the halo stars and the stars belonging to dwarf spheroidals can perhaps be reconciled if the Milky Way halo progenitors are biased towards

massive, early accretion events (Robertson et al. 2005; Font et al. 2006). The combination of high-mass and early accretion, can lead to abundance patterns (at least in the  $[\alpha/\text{Fe}]-[\text{Fe}/\text{H}]$  plane) similar to that exhibited by the present day halo stars. This scenario has been supported by recent evidence of a “break” in the stellar halo density profile at  $r \sim 25$  kpc (Deason et al. 2011; Sesar et al. 2011). In Deason et al. (2013), we argue that this break could be evidence for a major (relatively early) accretion event. However, this is not a unique solution; the same broken profile can plausibly be produced from multiple, but synchronized, lower-mass accretion events.

A different scenario posits that analogues of the “ultra-faint” dwarf galaxies could contribute significantly (at least at the metal-poor end) to the present-day stellar halo (e.g. Frebel et al. 2010; Clementini 2010). For example, Clementini (2010) argue that the Oosterhoff classification (Oosterhoff 1939) of RR Lyrae stars in ultra-faint dwarfs is in better agreement with the stellar halo compared to the more massive dwarfs<sup>1</sup>. Thus, an alternative view is that the stellar halo is built-up from a very large number of puny dwarfs. Finally, bear in mind that the characteristic building blocks of the stellar halo need not be dwarf galaxies. Previous work has argued

<sup>1</sup> However, we note that Fiorentino et al. (2014) recently showed that the period and luminosity amplitudes of RR Lyrae stars in the halo are more consistent with massive dwarfs (such as Sagittarius) than lower-mass dwarfs.

\* E-mail: alis@ucolick.org

that a significant fraction of the stellar halo (up to 50%) could be assembled from destroyed globular clusters (Carretta et al. 2010; Martell et al. 2011).

Despite the wealth of work attempting to decipher the mass spectrum of accreted substructures, we currently lack a clear picture of what made up the stellar halo, and when. In this letter, we use an alternative approach to gain insight into the progenitors of the Galactic halo. Recent work by Momany (2014) (see also Momany et al. 2007) showed that the number ratio of blue straggler (BS) to horizontal branch (HB) stars in dwarfs and globular clusters is dependent on the satellite’s stellar mass. Hence, this ratio could potentially be used to constrain the mass spectrum of substructures that contributed to the stellar halo. With this aim in mind, we provide a careful comparison between the number ratio of BS-to-blue horizontal branch (BHB) stars in different Milky Way companions (classical dwarfs, ultra-faint dwarfs and globular clusters) and the stellar halo overall.

## 2 A-TYPE STAR POPULATIONS IN THE MILKY WAY HALO

In this section, we identify the BHB and BS populations in dwarf galaxies, globular clusters and the stellar halo. Momany (2014) (also Momany et al. 2007) showed that the ratio of BS to HB stars varies as a function of luminosity for satellites in the Milky Way. However, in their study the entire HB was considered, which includes the red horizontal branch (RHB) and the extended blue tail of the HB. The RHB is notoriously difficult to identify in the stellar halo, and current BS-to-HB ratios in the stellar halo are upper limits as only BHB stars are included. Hence, in this work we consider the BS-to-BHB ratio for a fair comparison between satellites and the field halo. Our use of BHB stars on the denominator of this population ratio could be perceived as problematic, particularly if the BHB population is scarce, or does not exist at all in some satellites. However, it is worth pointing out that, to our knowledge, there isn’t a single dwarf galaxy that does not have any BHB stars. On the other hand, some very metal-rich globular clusters are devoid of a BHB population, and we discuss this further in Section 2.2.

We note that our choice of BS-to-BHB ratio as a probe of the stellar halo progenitors is made for both physical and practical reasons. The BS-to-BHB ratio is arguably the cleanest population relation that can be measured in both satellite galaxies and the stellar halo (see Section 2.3). In particular, redder populations such as RHB and red giant branch (RGB) stars suffer from severe foreground contamination, and are much more difficult to isolate in the halo with photometry alone. However, the main advantage of using these A-type star populations is that the BS-to-BHB *ratio* is easier to quantify in the stellar halo than the total number of BHB, BS, RGB, RHB etc. stars alone (see Deason et al. 2011 and Section 2.3).

### 2.1 Dwarf Galaxies

Our compilation of dwarf galaxies in the Milky Way is obtained from a variety of photometric data sources in the literature (see Table 1). We ensure that our sample only includes photometric data deep enough to reliably identify the BS population (typically  $\sim 2$  magnitudes fainter than BHBs) from the colour-magnitude diagram (CMD), and we only include datasets where  $N_{\text{BHB}} > 1$  and  $N_{\text{BS}} > 1$ . This excludes some of the more distant dwarfs without sufficiently deep photometry (e.g. Canes Venatici I), and some of the ultra-faint dwarfs with very few stars (e.g. Segue I).

Our dwarf sample excludes cases with known recent star formation (e.g. Fornax, Leo I, Carina - see e.g. Weisz et al. 2014), where contamination by young stars inhibits reliable estimates of the BS population. Very young stars ( $\sim 1 - 3$  Gyr, see e.g. Santana et al. 2013) can mimic BS stars in dwarf galaxies, and we are guided by the star formation histories derived in Weisz et al. (2014) to exclude these cases where possible. For consistency, we convert all magnitudes into SDSS bandpasses. Johnson-Cousins magnitudes are converted to *gri* SDSS filters using the relations in Jordi et al. (2006), and HST/ACS filters are converted into Johnson-Cousins bandpasses using the procedure outlined in Sirianni et al. (2005). The magnitudes and colours we use have been corrected for extinction following the prescription of Schlegel et al. (1998).

For a fair comparison with the stellar halo (see below), only A-type stars with  $-0.25 < g-r < 0$  are used. In cases where  $g-i$  colour is most appropriate (e.g. for *V*, *I* filters), we used bright A-type stars from SDSS ( $16 < g < 17$ ) to calibrate a linear relation between  $g-i$  and  $g-r$ . We find that the colour range  $-0.25 < g-r < 0.0$  roughly corresponds to  $-0.44 \lesssim g-i \lesssim -0.11$  for A-type stars. We use the globular cluster sample (see below) with *gri* photometry to ensure that our selection of A-type stars in  $g-i$  is consistent with our selection using  $g-r$ .

Some example CMDs are shown in Fig. 1. The selection region for BHB and BS stars are shown with the blue and red polygons, respectively. We use the Trilegal Galaxy model (Girardi et al. 2005) to estimate the foreground contamination included in our A-type star samples. The estimated foreground in the BHB and BS CMD selection regions is subtracted before the BS-to-BHB fractions are computed. Note that in some cases control-fields are available, and we use these to ensure that our estimated contamination from the Trilegal model is doing a reasonable job. In general, the contamination in the blue ( $g-r < 0$ ) region of CMD space probed in this work is minimal.

The resulting BS-to-BHB ratios are given in Table 1 and shown in Fig. 2. The quoted error estimates only include Poisson noise. For datasets where we are privy to the full photometric error distribution, we find that our measurements are not significantly affected by photometric uncertainties, and in most cases, the error budget is indeed dominated by number statistics. There are several unavoidable sources of error apparent when computing the BS-to-BHB ratio: (i) uncertain foreground/background subtraction; (ii) confusion between BS stars and normal main sequence stars; and, (iii) radial gradients in dwarfs. However, the general agreement between BS-to-BHB ratios from different data sources (different FOV, filters, sample size etc.) of *the same dwarf* is encouraging, and suggests that these potential systematic uncertainties are not significantly affecting our results. Where there are multiple data sources for the same dwarf we show the weighted (by inverse variance) mean value of  $N_{\text{BS}}/N_{\text{BHB}}$  in Fig. 2.

### 2.2 Globular Clusters

We also show in Fig. 2 the BS-to-BHB number ratio for globular clusters in the An et al. (2008) sample. These globular clusters have SDSS photometry and the BHB and BS populations are identified from the CMDs in the same way as the dwarf galaxies. We only include globular clusters with  $N_{\text{BHB}} > 1$  and  $N_{\text{BS}} > 1$ , and ensure that the photometry is deep enough to identify the BS population. This leaves a sample of 12 globular clusters that satisfy our requirements. An example of a globular cluster CMD is shown in the right-hand panel of Fig. 1.

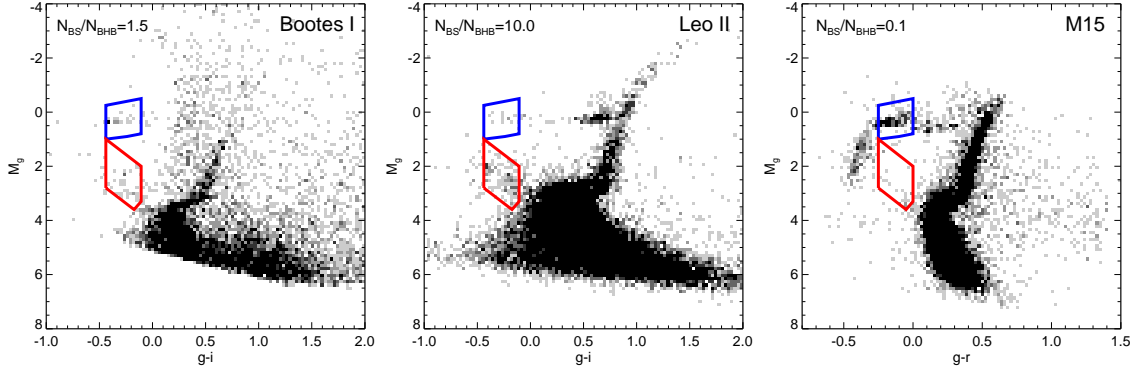


**Figure 1.** Three example colour-magnitude diagrams in  $gri$  SDSS filters, with original photometry from Belokurov et al. (2006), Held (2005) and An et al. (2008), respectively. The selection of BHB/BS stars are indicated with the blue/red lines, respectively.

Name	$M_V$	Photometry	FOV	$N_{BS}/N_{BHB}$	Ref	$\langle N_{BS}/N_{BHB} \rangle$
Boötes I	-6.3	Blanco/Mosaic-II ( $g, i$ )	$36' \times 36'$	$1.3 \pm 0.4$	B06	$1.5 \pm 0.5$
		Subaru/Suprime-Cam ( $V, I$ )	$34' \times 27'$	$2.5 \pm 0.9$	O12	
		HST/ACS (F606W, F814W)	$(5) 3.4' \times 2'$	$3.0 \pm 2.5$	W15	
Canes Venatici II	-4.9	Subaru/Suprime-Cam ( $g', i'$ )	$34' \times 27'$	$0.6 \pm 0.3$	B07	$0.6 \pm 0.2$
		HST/ACS (F606W, F814W)	$3.4' \times 2'$	$0.7 \pm 0.4$	W15	
		HST/WFPC2 (F606W, F814W)	$2.4' \times 2'$	$0.7 \pm 0.6$	H06	
Cetus	-11.2	HST/ACS (F475W, F814W)	$3.4' \times 2'$	$45.4 \pm 11.5$	M12	$45.4 \pm 11.5$
Coma Berenices	-4.1	Subaru/Suprime-Cam ( $g', i'$ )	$34' \times 27'$	$0.5 \pm 0.4$	B07	$0.5 \pm 0.4$
Draco	-8.8	INT/WFC ( $V, I$ )	$\sim 1 \text{ deg}^2$	$5.4 \pm 1.2$	A01	$5.3 \pm 1.1$
		HST/ACS (F555W, F814W)	$3.4' \times 2'$	$4.0 \pm 3.2$	W15	
Hercules	-6.6	HST/ACS (F606W, F814W)	$3.4' \times 2'$	$1.0 \pm 0.6$	W15	$1.0 \pm 0.6$
Leo II	-9.8	HST/WFPC2 (F555W, F814W)	$2.4' \times 2'$	$9.2 \pm 2.7$	H05	$10.0 \pm 1.9$
		HST/ACS (F555W, F814W)	$3.4' \times 2'$	$14.8 \pm 4.9$	W15	
		HST/WFPC2 (F606W, F814W)	$2.4' \times 2'$	$9.4 \pm 2.7$	H06	
Leo IV	-5.8	Subaru/Suprime-Cam ( $V, I$ )	$34' \times 27'$	$3.2 \pm 1.5$	O12	$1.7 \pm 1.0$
		HST/ACS (F606W, F814W)	$3.4' \times 2'$	$1.0 \pm 1.0$	W15	
Sagittarius	-13.5	MPI/WFI ( $V, I$ )	$\sim 1 \text{ deg}^2$	$10.0 \pm 1.0$	M03	$10.0 \pm 1.0$
Sculptor	-11.1	MPI/WFI ( $B, V, I$ )	$34' \times 33'$	$2.6 \pm 0.1$	R03	$2.0 \pm 0.4$
		CTIO/MOSAIC ( $V, I$ )	$\sim 4 \text{ deg}^2$	$1.8 \pm 0.1$	T11	
Sextans	-9.3	CFHT/CFH12K ( $B, V, I$ )	$42' \times 28'$	$6.2 \pm 1.1$	L03	$6.2 \pm 1.1$
Tucana	-9.5	HST/ACS (F475W, F814W)	$3.4' \times 2'$	$3.7 \pm 0.3$	M12	$3.7 \pm 0.3$
Ursa Major I	-5.5	Subaru/Suprime-Cam ( $V, I$ )	$34' \times 27'$	$0.3 \pm 0.2$	O12	$0.4 \pm 0.2$
		INT/WFC ( $B, r$ )	$23' \times 12'$	$1.5 \pm 1.0$	W05	
Ursa Minor	-8.8	INT/WFC ( $B, R$ )	$0.75 \text{ deg}^2$	$1.0 \pm 0.1$	C02	$1.0 \pm 0.1$
		HST/WFPC2 (F555W, F606W, F814W)	$(2) 2.4' \times 2'$	$2.3 \pm 1.0$	H06	

**Table 1.** The dwarf galaxies used in this work. We list the dwarf name, absolute visual magnitude, the photometry used to calculate population ratios, approximate FOV, BS-to-BHB number ratio, appropriate references to the photometric data sources, and (weighted) average BS-to-BHB number ratio. A01: Aparicio et al. (2001), B06: Belokurov et al. (2006), B07: Belokurov et al. (2007), C02: Carrera et al. (2002), H05: Held (2005), H06: Holtzman et al. (2006), L03: Lee et al. (2003), M03: Monaco et al. (2003), O12: Okamoto et al. (2012), R03: Rizzi et al. (2003), T11: de Boer et al. (2011), W15: Weisz et al. in prep., W05: Willman et al. (2005)

We note that we do not include the relatively metal-rich ( $[\text{Fe}/\text{H}] \gtrsim -0.8$ ) globular clusters that do not have a BHB population, but do have BS stars (see e.g. Piotto et al. 2002). These systems would boast abnormally high BS-to-BHB ratios and could potentially contribute BS stars to the halo. However, given the metal-poor nature of the stellar halo ( $\langle [\text{Fe}/\text{H}] \rangle \sim -1.5$ , Ivezić et al. 2008; An et al. 2013) it is reasonable to assume that these metal-rich globular clusters are not significant contributors.

### 2.3 Stellar Halo

The identification of BS and BHB stars in the stellar halo is not as straightforward. While at bright magnitudes ( $g \lesssim 18.5$ ), A-type stars can easily be distinguished from white dwarfs and quasars using  $ugr$  photometry, BS and BHB stars cannot be cleanly separated using photometry alone.

In Deason et al. (2011) (hereafter, DBE11), we used A-type stars selected from SDSS to measure the density profile of the stellar halo out to  $D \sim 40$  kpc. DBE11 took advantage of the overlap

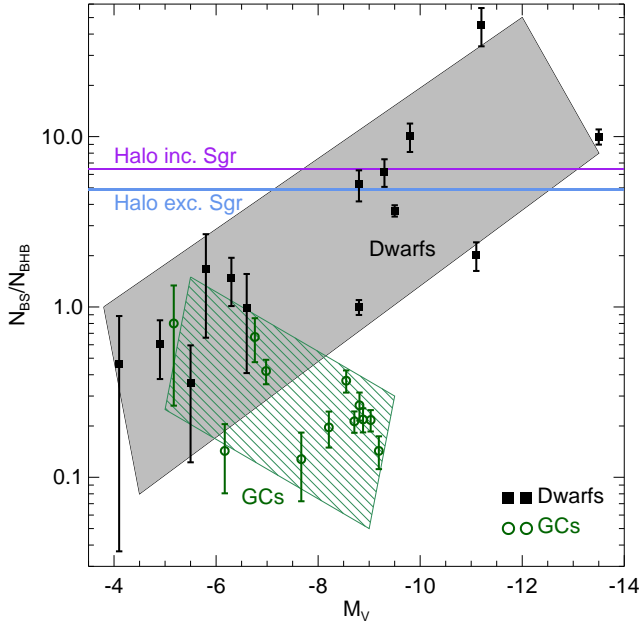


**Figure 2.** Number ratio of BS-to-BHB stars as a function of absolute visual magnitude. Dwarfs and globular clusters are shown with black squares and green circles, respectively. The quoted error bars only include Poisson noise. The halo number ratio is computed using the results of DBE11; the derived halo density profile is used to convert the overall number ratio (in a fixed magnitude slice) to a number ratio at fixed volume. The solid gray and line-filled green bands illustrate the correlation between  $N_{BS}/N_{BHB}$  and  $M_V$  for dwarfs and globular clusters, respectively.

ping, but distinct,  $ugr$  distributions of BS and BHB stars (see Fig. 2 in DBE11). The BHB and BS populations were modeled simultaneously with class probabilities based on  $ugr$  photometry alone. This method resulted in two quantities important for this work: 1) an estimate of the number ratio of BS-to-BHB stars in a fixed magnitude slice (see Table 1 in DBE11) and 2) a measure of the stellar halo density profile, under the assumption that both BHB and BS populations follow the same density profile.

In order to compare the stellar halo with the satellite populations, we must take into account the different volumes probed by BHB and BS stars in a fixed magnitude slice (BS stars are  $\sim 2$  mag fainter than BHB stars). Thus, we use the ratio  $\rho_{BS}^0/\rho_{BHB}^0$ , where  $\rho_{BS}^0 = N_{BS}/V_{BS}$  and  $\rho_{BHB}^0 = N_{BHB}/V_{BHB}$ . Here,  $N_{BS}$  and  $N_{BHB}$  are the numbers of BS and BHB stars in a fixed magnitude slice, and the volumes ( $V_{BS}, V_{BHB}$ ) are given by equation (9) in DBE11. The resulting ratios are  $4.9 \pm 0.1$  and  $6.4 \pm 0.1$  when stars belonging to the Sagittarius stream are excluded<sup>2</sup> or included, respectively. The error estimates take into account the different likelihoods of stellar halo density models. The halo ratios are shown with the purple and blue lines in Fig. 2.

### 3 POPULATION RATIOS: COMPARING SATELLITES WITH THE STELLAR HALO

Our compilation of BS-to-BHB number ratios for halo populations is shown in Fig. 2 as a function of absolute magnitude. Dwarfs and globular clusters are displayed with the solid black squares and

<sup>2</sup> Using the same mask defined in DBE11.

open green circles, respectively. The BS-to-BHB number ratios increase with luminosity for the dwarfs, but the opposite trend is seen for the globular clusters.

Momany (2014) showed that the BS-to-HB ratio for dwarfs *decreases* with absolute magnitude. We find the opposite trend for dwarf galaxies when only the BHB population is included on the denominator. This difference is because Momany (2014) includes *all* HB stars (BHB, RHB and the extended blue tail of the HB) in their analysis, so their trend is likely due to the more massive dwarfs having a more prominent RHB. As stated earlier, the RHB population is extremely difficult to quantify in the stellar halo, so the BS-to-BHB ratio provides a more robust comparison between satellites and halo stars.

The difference in trends shown for GCs and dwarf galaxies is likely related to the different BS formation mechanisms in these systems. The two main established routes of BS production (see e.g. Davies et al. 2004), from collisional-binaries and primordial, wide-binaries, have different significances in dwarfs and clusters; both formation channels act in globular clusters, whereas the low stellar density environments of dwarf galaxies precludes the occurrence of collisional binaries. Additionally, the higher densities (and collisional probabilities) in more massive globular clusters can lead to BS disruption (through 3-body interactions), but this process is not important for the (similar mass) dwarfs. This likely explains the large differences in  $N_{BS}/N_{BHB}$  fractions at  $M_V \sim -9$  between dwarfs and globular clusters.

The fainter dwarfs ( $M_V \gtrsim -7.5$ ) have similar BS-to-BHB number ratios to globular clusters at comparable luminosities, whereas more massive dwarfs have much higher ratios than globular clusters.

While the brighter Milky Way dwarfs have much larger BS-to-BHB number ratios than the fainter dwarfs, there is also a good deal of scatter. For example, Sculptor and Cetus have very similar absolute magnitudes ( $M_V \sim -11$ ) but very different number ratios,  $N_{BS}/N_{BHB} \sim 2$  for Sculptor and  $N_{BS}/N_{BHB} \sim 40$  for Cetus<sup>3</sup>. The star formation histories of these two dwarfs derived by Weisz et al. (2014) from *HST* photometry are also very different, where Sculptor has a much older stellar population. It is clear that at fixed luminosity the star formation histories (and hence BS-to-BHB number ratios) can vary substantially, especially for more massive dwarfs.

Despite the large scatter for bright dwarfs, it is clear that the low BS-to-BHB number ratios for ultra-faint dwarfs ( $N_{BS}/N_{BHB} \sim 1$ ) and globular clusters ( $N_{BS}/N_{BHB} < 1$ ) are *not compatible with the relatively high BS-to-BHB ratio in the Milky Way stellar halo*. Thus, it is unlikely that the bulk of the stellar halo was built up from (a very large number of) low luminosity systems such as ultra-faint dwarfs and/or globular clusters. This is in agreement with the current model predictions from  $\Lambda$ CDM simulations, postulating that stellar halos are generally dominated by massive accretion events (Bullock & Johnston 2005; Cooper et al. 2010; Deason et al. 2013). We do note, however, that if the progenitor satellites were drastically different to the surviving populations today, then we must be more circumspect regarding our comparison with halo stars. For example, globular clusters destroyed a long time ago ( $\sim 10$  Gyr) may not have had time for collisional processes to occur, and thus the BS population may be very dif-

<sup>3</sup> The unusually high BS-to-BHB number ratio in Cetus may result from contamination by young (1 – 2 Gyr) stars. Yet, to our knowledge, there is no evidence for such population in the dwarf.



ferent in these proto-clusters. On the other hand, recent work by Brown et al. (2012) arguing that the UF-dwarfs are predominantly ancient ( $\sim 12 - 14$  Gyr) populations, suggests that we are not significantly biased when comparing with the “survivors” at these low mass-scales.

#### 4 CONCLUSIONS

In this Letter, we compiled a sample of BS and BHB stars in dwarf galaxies, globular clusters and the Milky Way stellar halo with the aim of comparing the BS-to-BHB ratio for different halo populations. We ensure that our selection of BS and BHB stars is as consistent as possible (i.e. using the same photometric system and colour cuts) between different datasets, and correct the approximate number ratio of BS-to-BHB stars in the stellar halo (at fixed magnitude slice) for volume effects. Our main conclusions are as follows:

- The number ratio of BS-to-BHB stars in dwarf galaxies increases with increasing luminosity. Ultra-faint dwarfs have  $N_{BS}/N_{BHB} \sim 1$ , while more massive dwarfs can range from  $N_{BS}/N_{BHB} \sim 2$  to  $N_{BS}/N_{BHB} \sim 40$ . The large scatter for more massive dwarfs is probably due to the wide variation in star formation histories.

- GCs tend to have low BS-to-BHB ratios,  $N_{BS}/N_{BHB} \lesssim 1$ , which *decreases* with increasing luminosity. The different trends shown by globular clusters and dwarfs likely reflect the different formation mechanisms of BS stars in these two populations (see e.g. Santana et al. 2013; Momany 2014).

- The relatively high BS-to-BHB ratio in the stellar halo ( $N_{BS}/N_{BHB} \sim 5 - 6$ ) is inconsistent with the low ratios found for ultra-faint dwarfs and globular clusters. This result argues against ultra-faints and globular clusters being the dominant “building blocks” of the stellar halo, and instead favours more massive dwarfs as the more predominant progenitors.

#### ACKNOWLEDGMENTS

We thank Yazan Momany, Mateo Monelli, Sakurako Okamoto and Myung Goon Lee for kindly sharing their photometric data with us. We also thank Francesca De Angeli, Yazan Momany and an anonymous referee for providing useful comments on the paper. AJD and DRW are currently supported by NASA through Hubble Fellowship grants HST-HF-51302.01,51331.01, awarded by the Space Telescope Science Institute, which is operated by the Association of Universities for Research in Astronomy, Inc., for NASA, under contract NAS5-26555. We thank the Aspen Center for Physics and the NSF Grant #1066293 for hospitality during the conception of this paper. The research leading to these results has received funding from the European Research Council under the European Union’s Seventh Framework Programme (FP/2007-2013) / ERC Grant Agreement n. 308024.

#### REFERENCES

An D., et al., 2008, ApJS, 179, 326  
 An D., et al., 2013, ApJ, 763, 65  
 Aparicio A., Carrera R., Martínez-Delgado D., 2001, AJ, 122, 2524  
 Belokurov V., et al., 2006, ApJ, 647, L111  
 Belokurov V., et al., 2007, ApJ, 654, 897

Brown T. M., et al., 2012, ApJ, 753, L21  
 Bullock J. S., Johnston K. V., 2005, ApJ, 635, 931  
 Carrera R., Aparicio A., Martínez-Delgado D., Alonso-García J., 2002, AJ, 123, 3199  
 Carretta E., Bragaglia A., Gratton R. G., Recio-Blanco A., Lucatello S., D’Orazi V., Cassisi S., 2010, A&A, 516, A55  
 Clementini, G. 2010, in Variable Stars, the Galactic halo and Galaxy Formation, eds. C. Sterken, N. Samus, & L. Szabados (Moscow: Sternberg Astronomical Institute of Moscow Univ.), 107  
 Cooper A. P., et al., 2010, MNRAS, 406, 744  
 Davies M. B., Piotto G., de Angeli F., 2004, MNRAS, 349, 129  
 Deason A. J., Belokurov V., Evans N. W., 2011, MNRAS, 416, 2903  
 Deason A. J., Belokurov V., Evans N. W., Johnston K. V., 2013, ApJ, 763, 113  
 de Boer T. J. L., et al., 2011, A&A, 528, A119  
 Fiorentino, G., et al., 2014, ApJL in press, arXiv:1411.7300  
 Font A. S., Johnston K. V., Bullock J. S., Robertson B. E., 2006, ApJ, 646, 886  
 Frebel A., Simon J. D., Geha M., Willman B., 2010, ApJ, 708, 560  
 Girardi L., Groenewegen M. A. T., Hatziminaoglou E., da Costa L., 2005, A&A, 436, 895  
 Held, E. V., 2005, in IAU Colloq. 198: Near-field cosmology with dwarf elliptical galaxies, eds. Jerjen H., Binggeli B., 11  
 Holtzman J. A., Afonso C., Dolphin A., 2006, ApJS, 166, 534  
 Ivezić Ž., et al., 2008, ApJ, 684, 287  
 Jordi K., Grebel E. K., Ammon K., 2006, A&A, 460, 339  
 Lee M. G., et al., 2003, AJ, 126, 2840  
 Martell S. L., Smolinski J. P., Beers T. C., Grebel E. K., 2011, A&A, 534, A136  
 Momany Y., Held E. V., Saviane I., Zaggia S., Rizzi L., Gullieszik M., 2007, A&A, 468, 973  
 Momany Y., 2014, in Ecology of Blue Straggler Stars (Ch6), eds. H.M.J. Boffin, G. Carraro & G. Beccari, Astrophysics and Space Science Library, Springer  
 Monaco L., Bellazzini M., Ferraro F. R., Pancino E., 2003, ApJ, 597, L25  
 Okamoto S., Arimoto N., Yamada Y., Onodera M., 2012, ApJ, 744, 96  
 Oosterhoff P. T., 1939, The Observatory, 62, 104  
 Piotto G., et al., 2002, A&A, 391, 945  
 Rizzi L., Held E. V., Momany Y., Saviane I., Bertelli G., Moretti A., 2003, Mem. Soc. Astron. Italiana, 74, 510  
 Robertson B., Bullock J. S., Font A. S., Johnston K. V., Hernquist L., 2005, ApJ, 632, 872  
 Santana F. A., Muñoz R. R., Geha M., Côté P., Stetson P., Simon J. D., Djorgovski S. G., 2013, ApJ, 774, 106  
 Schlegel D. J., Finkbeiner D. P., Davis M., 1998, ApJ, 500, 525  
 Sesar B., Jurić M., Ivezić Ž., 2011, ApJ, 731, 4  
 Sirianni M., et al., 2005, PASP, 117, 1049  
 Tolstoy E., Venn K. A., Shetrone M., Primas F., Hill V., Kaufer A., Szeifert T., 2003, AJ, 125, 707  
 Venn K. A., Irwin M., Shetrone M. D., Tout C. A., Hill V., Tolstoy E., 2004, AJ, 128, 1177  
 Weisz D. R., Dolphin A. E., Skillman E. D., Holtzman J., Gilbert K. M., Dalcanton J. J., Williams B. F., 2014, ApJ, 789, 147  
 Willman B., et al., 2005, ApJ, 626, L85